Accepted Manuscript

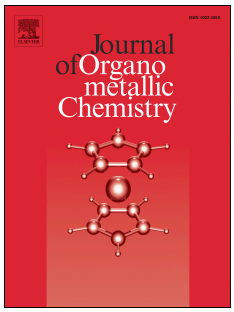

Synthesis, X-ray structures and anticancer activity of gold(I)-carbene complexes with selenones as co-ligands and their molecular docking studies with thioredoxin reductase

Adam A.A. Seliman, Muhammad Altaf, Abdulmujeeb T. Onawole, Saeed Ahmad, Mohammed Yagoub Ahmed, Abdulaziz Al-Saadi, Saleh Altuwaijri, Gaurav Bhatia, Jatinder Singh, Anvarhusein A. Isab

PII: S0022-328X(17)30464-3

DOI: 10.1016/j.jorganchem.2017.07.034

Reference: JOM 20048

To appear in: *Journal of Organometallic Chemistry*

Received Date: 27 April 2017

Revised Date: 25 July 2017

Accepted Date: 27 July 2017

Please cite this article as: A.A.A. Seliman, M. Altaf, A.T. Onawole, S. Ahmad, M.Y. Ahmed, A. Al-Saadi, S. Altuwaijri, G. Bhatia, J. Singh, A.A. Isab, Synthesis, X-ray structures and anticancer activity of gold(I)-carbene complexes with selenones as co-ligands and their molecular docking studies with thioredoxin reductase, *Journal of Organometallic Chemistry* (2017), doi: 10.1016/j.jorganchem.2017.07.034.

Two new linear gold(I) complexes of [Au(IPr)(Selenone)]PF_6 have been prepared. The structure of these complexes have been determined by single X-ray crystallography.

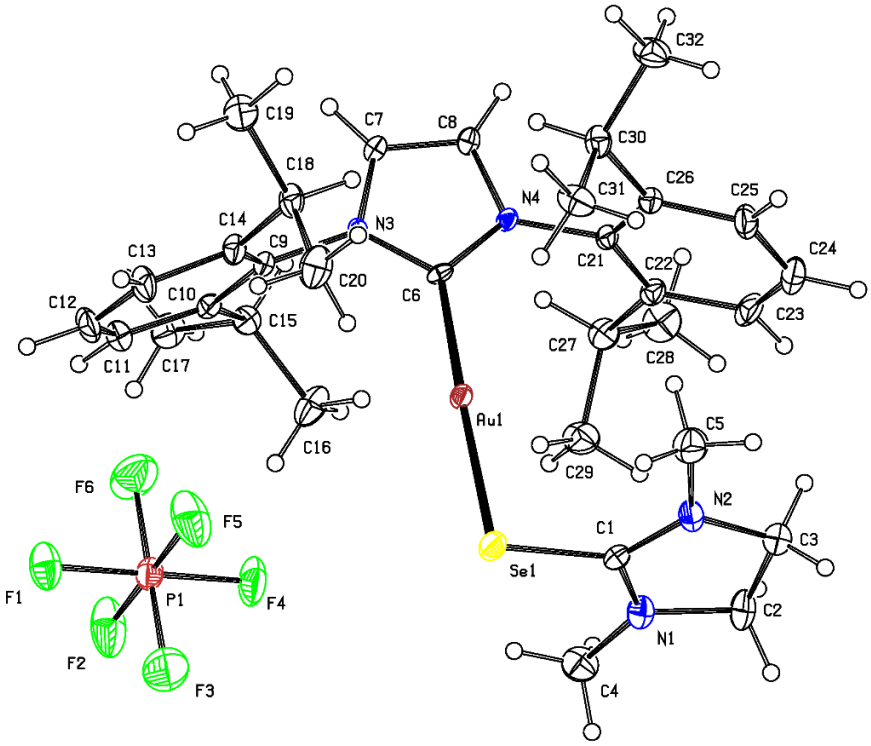

Synthesis, X-ray structures and anticancer activity of gold(I)-carbene complexes with selenones as co-ligands and their molecular docking studies with thioredoxin reductase

Adam A. A. Seliman[a,b], Muhammad Altaf[c], Abdulmujeeb T. Onawole[a], Saeed Ahmad[d], Mohammed Yagoub Ahmed[a], Abdulaziz Al-Saadi[a], Saleh Altuwaijri[e] Gaurav Bhatia[f] and Jatinder Singh[f] Anvarhusein A. Isab[a*]

[a]Department of Chemistry, King Fahd University of Petroleum and Minerals, Dhahran 31261, Saudi Arabia

[b]Department of Chemistry, Al-Neelain University, Khartoum 11121, Sudan.

[c]Center of Excellence in Nanotechnology, King Fahd University of Petroleum & Minerals, 31261 Dhahran 31261, Saudi Arabia.

[d]Department of Chemistry, College of Sciences and Humanities, Prince Sattam bin Abdulaziz University, Al-Kharj 11942, Saudi Arabia

[e]Clinical Research Laboratory, SAAD Research and Development Center, SAAD Specialist Hospital, Al-Khobar 31952, Saudi Arabia

[f] Department of Molecular, Biology & Biochemistry, Guru Nanak Dev University, Amritsar-143005, India

*Corresponding author: aisab@kfupm.edu.sa

Abstract

Five new gold(I) complexes of carbene and selenone ligands (**1**-**5**) having the general formula, [Au(IPr)(selenone)]PF_6 were synthesized by the reaction of [Au(IPr)Cl] (**0**) with selenones (where IPr = 1,3-Bis(2,6-di-isopropylphenyl)imidazol-2-ylidene and selenone = 1,3-imidazolidine-2-selenone, *N*-ethyl-1,3-imidazolidine-2-selenone, *N*-propyl-1,3-imidazolidine-2-selenone, *N*,*N*′-dimethyl-1,3-imidazolidine-2-selenone and *N*,*N*′-diethyl-1,3-imidiazolidine-2-selenone for **1**-**5** respectively. The complexes were characterized by elemental analysis, IR and NMR (^{1}H, ^{13}C, ^{77}Se) spectroscopy and two of them by X-ray crystallography. The X-ray diffraction analysis of complexes **2** and **4** revealed that they were composed of $[Au(IPr)(Selenone)]^{+}$ and PF_6^{-} ions. In the complex ions, gold(I) atom adopts a linear geometry. *In vitro* cytotoxicity was appraised for all complexes against HCT15, A549 and MCF7 cancer cell lines. The IC_{50} values showed that the complexes exhibited poor activity as compared to cisplatin. However, the complex **1** showed a promising anticancer activity (IC_{50} = 33 ± 1 μM) similar to that exhibited by cisplatin (32 ± 2 μM) against HCT15 (human colon cancer) cell line. The molecular docking analysis showed the potential inhibitory capacity of the gold complexes with thioredoxin reductase with complex **2** having the highest binding affinity with a score of -40.78. The interactions of the gold complexes with tryptophan and lysozyme were studied electrochemically using Cyclic and Square Wave Voltammetry.

Keywords: Gold(I)-carbene complexes, 1,3-imidazolidine-2-selenone; thioredoxin reductase; cytotoxicity; molecular docking.

1. Introduction

Gold(I) compounds have been used for the treatment of rheumatoid arthritis since 1930s [1,2]. The clinically used anti-arthritis gold(I) complexes include; gold(I) thiomalate (Myocrisin), gold(I) thioglucose (Solganol) and (2,3,4,6-tetra-O-acetyl-1-(thio-kS)-b-D-glucopyranosato)-(triethylphosphine)gold(I) (auranofin) [2-4]. In addition to their anti-arthritic properties, gold(I) complexes have appeared as very potent anticancer agents [5-27]; the most famous example being auranofin, which is in clinical trials for the treatment of several types of cancer [5,6]. Among the anticancer gold(I) complexes, the complexes of *N*-heterocyclic carbenes (NHCs) have been intensively investigated in recent years [13-27].

Preliminary studies on the mode of action of gold(I) complexes show that they mainly act through inhibition of mitochondrial enzymes including thioredoxin reductase (TrxR) [15,18-20,28-30]. TrxR inhibition determines a shift to the oxidized forms of Trx and Prx III (Peroxiredoxin 3), allowing a large increase in reactive oxygen species (ROS). The elevation of ROS causes oxidative stress in tumor cells, and is thus associated with the induction of apoptosis in the cells [29-31]. A novel series of Ru(II)- and Au(I)- *N*-heterocyclic carbenes have been recently reported and their *in vitro* cytotoxicity were tested against a panel of cancer cell lines. Among them, NHC─Au─Cl and NHC─Au─SR were tested for *in vivo* investigations in mice and the mode of action of both compounds induced TrxR inhibition through elevating oxidative stress [32,33].

The most commonly studied gold(I)-NHC complexes are those derived from imidazolium and benzimidazolium salts. In these complexes, carbene ligands usually bind through C2 carbon of imidazole [14-39]. However, in some cases, C2 is protected and carbene coordinates through another carbon atom [40,41]. The carbene ligands confer a high stability to the resulting gold compounds due to their ability to form strong coordinate covalent bonds through σ-donation (although, they are relatively weak π-acceptors) [42-44]. Their greater stability makes the metal–NHC complexes promising candidates for drug development. The binding of a soft selenium ligand to gold(I) trans to a carbene ligand could very likely give extra stability to the resulting compounds. Gold complexes of selenium donor ligands have been the focus of our research program for some time [45-50]. In this study, we have extended our investigation towards the synthesis, spectral as well as structural characterization and evaluation of anticancer properties of

gold(I) complexes of heterocyclic selenone containing a carbene as a co-ligand (**1**-**5**). To the best of our knowledge this is the first report describing the cytotoxic studies of such complexes. The structures of the ligands and the scheme for the synthesis of complexes along with the resonance assignments are given in scheme 1.

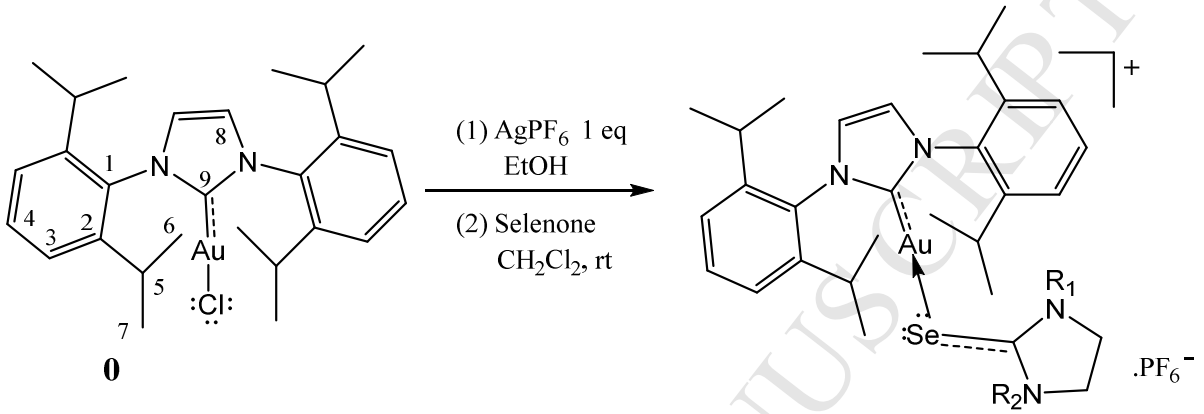

0

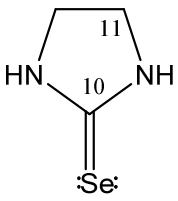

1

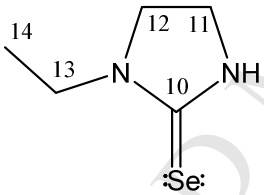

2

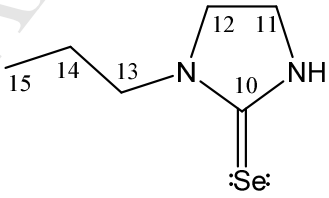

3

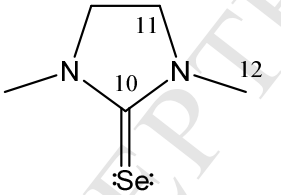

4

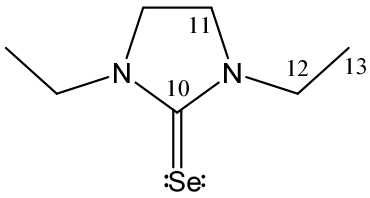

5

(1) 1,3-Imidazolidine-2-selenone (ImSe)

(2) *N*-ethyl-1,3-imidazolidine-2-selenone (EtImSe)

(3) *N*-propyl-1,3-imidazolidine-2-selenone (PrImSe)

(4) *N,N'*-dimethyl-1,3-imidazolidine-2-selenone (Me_2ImSe)

(5) *N,N'*-diethyl-1,3-imidazolidine-2-selenone (Et_2ImSe)

Scheme 1 Synthesis of gold(I)-selenone complexes (**1-5**) and structures of the ligands.

2. Experimental section

2.1. Chemicals

1,3-bis(2,6-di-isopropylphenyl)imidazol-2-ylidenegold(I)chloride ([Au(Ipr)Cl]), $AgPF_6$ lysozyme, tryptophan, ethanol, sodium dihydrogen phosphate and disodium hydrogen phosphate were purchased from Sigma-Aldrich Company, St. Louis, Missouri, USA. ImSe and its derivatives were synthesized according to methods reported in the literature [51,52]. Human colon cancer, human breast cancer and human lung cancer cell lines were purchased from National Centre for Cell Sciences (NCCS), Pune India. The double distilled water was used throughout the experiment and for solutions preparation. The double distilled water was collected from Lab based Water Still Aquatron A 4000 D unit.

2.2. Instrumentation

Elemental analysis was performed on Perkin Elmer Series 11(CHNS/O), Analyzer 2400. The solid state FTIR spectra were recorded on a Perkin-Elmer FTIR 180 spectrophotometer using KBr pellets over the range 4000-400 cm^{-1} at a resolution 4 cm^{-1}. The ^{1}H (500.01 MHz), ^{13}C (125.65 MHz) and ^{77}Se (200.0 MHz) NMR spectra were recorded on a LAMBDA 500 MHz NMR spectrophotometer. The ^{1}H and ^{13}C chemical shifts were referenced with respect to Tetramethylsilane (TMS), while for ^{77}Se NMR, $NaHSeO_3$ (1308 ppm) was used as an external standard. The ^{13}C (MAS) NMR results were recorded on a Bruker 400.0 MHz spectrometer at the ambient room temperature of 298 K. Samples were packed into 4 mm zirconium oxide rotors. A pulse delay of 7.0 s and a contact time of 5.0 ms. The magic angle spinning rates were

4 and 8 kHz. Carbon-13 chemical shifts were measured relative to adamantine, which resonate at 38.56 ppm.

The X-ray data for complexes **2** and **4** was collected at 173K on a STOE IPSD II Image Plate Diffraction System connected with a two-circle goniometer and using Mo*K*α graphite monochromator (λ= 0.71073 Å). The structures were solved by SHELXS-2014 program [53]. The refinement and further calculations were carried out with SHELXL-2014 [54]. The NH H atoms were located in a Difference Fourier map and refined with a distance restraint of N-H = 0.88(2) Å and H…H = 1.40(2) Å. The C-bound H-atoms were included in calculated positions and treated as riding atoms: C-H = 0.95 - 1.0 Å with $U_{iso}(H) = 1.5U_{eq}(C)$ for methyl H atoms and $= 1.2U_{eq}(C)$ for other H-atoms. The non-H atoms were refined anisotropically, using weighted full-matrix least squares on F^2. A semi-empirical absorption correction was applied using the MULscanABS routine in PLATON [55]. The crystal data and refinement details are given in Table S1.

The cyclic and the square wave voltammetric measurements were performed using Auto Lab (Netherland). The voltammetric measurements were done using three electrode systems. The glassy carbon electrode, platinum, and Ag/AgCl were used as working, counter and a reference electrode, respectively. The weights of the various chemicals were measured using GR-2000. The Accumet® XL50 pH meter was used for the monitoring of buffer pH.

2.3. Measurement of Anticancer Activity

The cells were seeded at 3 x 10^3 cells/well in 100 μL of DMEM containing 10% fetal bovine serum (FBS) in a 96-well tissue culture plate and incubated for 72 h at 37 ^oC, 5% CO_2 and 90% relative humidity in a CO_2 incubator. After incubation, 100 μL of 100, 50, 25 and 12.5 μM solutions of cisplatin and gold(I) complexes prepared in Dulbecco's Modified Eagle's Medium (DMEM), was added to the cells and the cultures were incubated for 24 h. The medium in the wells was casted off and 100 μL of DMEM containing MTT (0.5 mg/ml) was added to the wells, with subsequent incubation in the CO_2 incubator at 37 ^{o} C in the dark for 4 h. After incubation, purple-colored formazan produced by the cells appeared as dark crystals in the bottom of the wells. The culture medium was carefully removed from each well to prevent disruption of the monolayer and 100 μL of dimethyl sulfoxide (DMSO) was added to each well.

The solution in the wells was thoroughly mixed to dissolve the formazan crystals which produce a purple solution. The absorbance of the 96 well-plates was measured at 570 nm with Labsystems Multiskan EX ELISA reader against a reagent blank. The experimental results are calculated as the micromolar concentration of 50% cell growth inhibition (IC_{50}) of each drug. The MTT assay was carried out in three independent experiments, each in triplicate.

2.4. Synthesis of gold(I) complexes

To 0.127 g (0.500 mmol) $AgPF_6$ in 5.0 mL ethanol was added 0.311 g (0.500 mmol) chlorido[1,3-Bis(2,6-diisopropylphenyl)imidazol-2-ylidene]gold(I), [Au(IPr)(Cl)] dissolved in 15.0 mL of CH_2Cl_2. After stirring for 5 minutes at room temperature, the solution was filtered. To the filtrate, 0.500 mmol selenone (1,3-imidazolidine-2-selenone or its derivative) was added. The solution was stirred for 1 hour, filtered and then kept in the refrigerator for crystallization. After three to four days the products were separated. The complexes **1**, **3** and **5** were separated as white, gray and yellow powdered solids respectively. The compounds **2** and **4** were obtained as grayish white crystals respectively.

2.5. Analytical and Spectroscopic Data

[Au(IPr)(ImSe]PF_6 (**1**), Calc. for $C_{30}H_{42}AuF_6PN_4Se$, Mw = 879.57 g/mol: C, 40.97; H, 4.81; N, 6.37. Found: C, 41.38; H, 4.64; N, 6.28. Yield = 0.248 g (56%). ^{1}H NMR ($CDCl_3$, ppm): δ 8.85 (NH, s, 2H), 7.39 (C3-H, d, 2H), 7.57 (C4-H, t, 2H), 2.56 (C5-H, m, 4H), 1.33 (C6-H, d, 12H), 1.28 (C7-H, s, 12H), 7.65 (C8-H, s, 2H), 3.60 (C11-H, s, 4H). ^{13}C NMR ($CDCl_3$, ppm): δ 145.1 C(1), 132.7 C(2), 123.2 C(3), 130.0 C(4), 27.8 C(5), 23.5 C(6), 23.0 C(7), 123.4 C(8), 181.6 C-Au, 168.7 C=Se, 44.8 C(11). ^{77}Se NMR ($CDCl_3$, ppm): δ 42.80.

[Au(IPr)(EtImSe]PF_6 (**2**), Calc. for $C_{32}H_{46}AuF_6N_4PSe$, Mw = 907.62 g/mol: C, 42.39; H, 5.11; N, 6.18. Found: C, 42.43; H, 5.83; N, 6.46. Yield = 0.264 g (60%). ^{1}H NMR ($CDCl_3$, ppm): δ 8.95 (NH, s, 1H), 7.36 (C3-H, d, 2H), 7.61 (C4-H, t, 2H), 2.54 (C5-H, m, 4H), 1.31 (C6-H_3, d, 12H), 1.26 (C7-H, s, 12H), 7.33 (C8-H, s, 2H), 3.46 (C11-H, m, 2H), 3.54 (C12-H, m, 2H), 3.76 (C13-H, m, 2H), 1.15 (C14-H, m, 3H). ^{13}C NMR ($CDCl_3$, ppm): δ 145.9 C(1), 133.5 C(2), 123.9 C(3), 131.3 C(4), 28.8 C(5), 24.4 C(6), 23.9 C(7), 124.4 C(8), 182.0 C-Au, 171.8 C=Se, 43.9 C(11), 49.0 C(12), 43.4 C(13), 12.0 C(14). ^{77}Se NMR ($CDCl_3$, ppm): δ 75.36.

[Au(IPr)(PrImSe]PF_6 (**3**), Calc. for $C_{33}H_{48}AuF_6PN4Se$, Mw = 921.65g/mol: C, 43.05; H, 5.25; N, 6.09. Found: C, 42.57; H, 5.51; N, 5.81. Yield = 0.240 g (55%). ^{1}H NMR ($CDCl_3$, ppm): δ 9.02 (NH, s, 1H), 7.38 (C3-H, d, 2H), 7.62 (C4-H, t, 2H), 2.55 (C5-H, m, 4H), 1.31 (C6-H, d, 12H), 1.26 (C7-H, s, 12H), 7.37 (C8-H, s, 2H), 3.76 (C11-H_2, t, 2H), 3.48 (C12-H, t, 2H), 3.28 (C13-H, t, 2H), 1.56 (C14-H, m, 2H), 0.86 (C15-H, t, 3H). ^{13}C NMR ($CDCl_3$, ppm): δ 146.0 C(1), 133.5 C(2), 123.9 C(3), 131.2 C(4), 28.8 C(5), 24.5 C(6), 23.9 C(7), 124.4 C(8), 182.4 C=Au, 170.5 C=Se, 43.6 C(11), 49.7 C(12), 50.7 C(13), 20.2 C(14), 10.9 C(15). ^{77}Se NMR ($CDCl_3$, ppm) δ 79.40.

[Au(IPr)(Me_2ImSe]PF_6 (**4**), Calc. for $C_{32}H_{46}Au\ F_6PN_4Se$, Mw = 907.63 g/mol: C, 42.39; H, 5.11; N, 6.18. Found: C, 42.68; H, 5.21; N 5.91. Yield = 0.265 g (60%). ^{1}H NMR ($CDCl_3$, ppm): δ 8.92 (C3-H, d, 2H), 7.59 (C4-H, t, 2H), 2.51 (C5-H, m, 4H), 1.26 (C6-H, d, 12H), 1.25 (C7-H, s, 12H), 7.30 (C8-H, s, 2H), 3.55 (C11-H, s, 2H), 2.85 (C12-H, s, 6H). ^{13}C NMR ($CDCl_3$, ppm): δ 141.7 C(1), 133.3 C(2), 123.7 C(3), 131.2 C(4), 28.8 C(5), 24.4 C(6), 23.9 C(7), 123.7 C(8), 181.3 C=Au, 170.4 C=Se, 49.9 C(11), 36.5 C(12). ^{77}Se NMR ($CDCl_3$, ppm): δ 88.44.

[Au(IPr)(Et_2ImSe]PF_6 (**5**), Calc. for $C_{34}H_{50}Au\ F_6PN_4Se$, Mw = 935.68 g/mol: C, 43.64; H, 5.39; N, 5.99. Found: C, 43.19; H, 5.71; N, 5.49. Yield = 0.284 g (61%). ^{1}H NMR ($CDCl_3$, ppm): δ 7.41 (C3-H, d, 2H); 7.61 (C4-H, t, 2H), 2.51 (C5-H, m, 4H), 1.31 (C6-H, d, 12H), 1.25 (C7-H, d, 12H), 7.31 (C8-H, s, 2H), 3.49 (C11-H, d, 2H); 3.75 (C12-H_2, t, 2H), 1.23 (C13-H, dd, 2H). ^{13}C NMR ($CDCl_3$, ppm): δ 145.6 C(1), 133.5 C(2), 123.9 C(3), 131.1 C(4), 28.8 C(5), 24.5 C(6), 23.9 C(7), 124.4 C(8), 182.2 C=Au, 167.2 C=Se, 44.2 C(11), 47.0 C(12), 12.0 C(13). ^{77}Se NMR ($CDCl_3$, ppm): δ 101.43.

2.6 Electrochemical measurements

The solutions of the complexes were prepared using ethanol as a solvent due to their good solubility in ethanol. Prior to every electrochemical measurement, the GCE was polished as a mirror-like surface on rubbing the synthetic cloth using the alumina slurry. Interaction of the anticancer compounds and the biomolecules were investigated using cyclic voltammetry and the square wave voltammetry. The cyclic and square wave voltammetry were scanned from 0.0 to +1.0 and -0.1 to +1.3 V, respectively.

3. Results and discussion

3.1. Spectroscopic characterization

The complexes **1-5** were prepared according to Scheme 1. The IR frequencies of the free ligands and their gold(I) complexes are summarized in Table 2S. The ν(C=Se) absorption band of the selenones observed in the range of 578-636 cm^{-1} was decreased to a lower frequency in the range of 554-557) cm^{-1} upon complexation. This significant shift rationalizes the formation of the complexes. On the other hand, the ν(N─H) stretching band was shifted towards the higher frequency region in complexes relative to the free ligands. This shift may be related to an increase in π character of the C─N bond upon complexation. Similar shifts have been observed for other gold(I) complexes of selenones [46-50].

The ^{1}H and ^{13}C solution NMR spectral data are given in the experimental section. The values for [Au(IPr)Cl] are in accordance with the reported literature [38]. In ^{1}H NMR the N-H signals of selenones shifted downfield as compared to their values in the free state. The deshielding is related to an increase in π character of the C–N bond due to the flow of electron density from nitrogen towards selenium upon coordination. In ^{13}C NMR chemical shifts of carbenic (C=Au) and C=Se carbon atoms of selenones are given in Table 3S. The carbene carbon resonance shifted downfield by more than 6 ppm with respect to its position in the precursor complex, [Au(IPr)Cl]. The downfield shift is consistent with the transfer of electron density from carbon to metal atom upon coordination. The other resonances of IPr ligand remained almost unaffected. On the other hand, the C=Se resonances in [Au(IPr)(Selenone)]PF_6 complexes appeared upfield by more than 6 ppm compared to those in uncoordinated selenones. This upfield shift is in accordance with the literature data [46-50].

The ^{77}Se NMR chemical shifts of free ligands and complexes (**1-5**) are given in Table 4S. In ^{77}Se NMR an upfield shift of 5.5-30.7 ppm was observed for all the ligands upon complexation. The upfield shift is related to the binding of selenium to a metal atom. This observation is consistent with the data of our previous studies [56,57]. The greatest shift was observed for the ImSe complex. As the shift difference, may be related to the stability of the

234 complexes, therefore, the ImSe complex is expected to be the most stable among these
235 complexes.

236 The solid state ^{13}C chemical shifts of all complexes showed consistency with those in the
237 liquid state. This observation indicates the similarity of environments of the carbon atoms in both
238 the solid and liquid states and hence marks the stability of the synthesized complexes in the solid
239 as well as the liquid state. The ^{13}C (MAS) NMR Chemical Shifts of complexes (**0-5**) are given in
240 Table 5S.

3.2. Crystal Structure Description

The molecular structures of [Au(IPr)(EtImSe]PF_6 (**2**) and [Au(IPr)(Me_2ImSe]PF_6 (**4**) are depicted in Figures 1 and 2 respectively. The selected bond lengths and bond angles are given in Table 1. Both compounds crystallized as ionic species consisting of [Au(IPr)(selenone)]$^+$ and PF_6^- ions. In the cationic complexes, the coordination geometry around the gold(I) ion is close to linear with the C—Au—Se bond angles of 176.82(6)^o and 176.76(17)^o for **2** and **4** respectively. These values reflect that the geometry at gold is somewhat distorted linear. The compounds **2** and **4** are isostructural and possess similar bond parameters. The Au—C and Au—Se bond lengths of the two complexes are of the same magnitude as those found in other gold(I) compounds of carbene [22-38] and selenone [58,59] ligands. The Au—C bond lengths of the complexes are 2.009(2) and 2.015(6) respectively. The bond connection about selenium is V-shaped (Au1—Se1—C1 95.30(2)^o or 98.62(8)^o) as observed previously [58,59]. The bond angles around >C=Se and carbene carbon atoms represent a trigonal planar environment. Similar to the gold(I) complexes of IPr-based selenones [58], no evidence of aurophilic interactions was found in the crystal structures of **2** and **4**, presumably due to the steric bulk of the IPr and selenones. In complexes of small-sized ligands, such as [Me_3P-Au-Seu]$_2Cl_2$ (Me_3P = Trimethylphosphine, Seu = selenourea) the aurophilic interactions (Au-Au = 3.0386(5) Å) favor the formation of a dinuclear complex [49]. In the case of **1**, the dimerization is probably hindered by the steric effect of the bulky ligands. The complex cations and PF_6^- anions are associated to each other through electrostatic interactions.

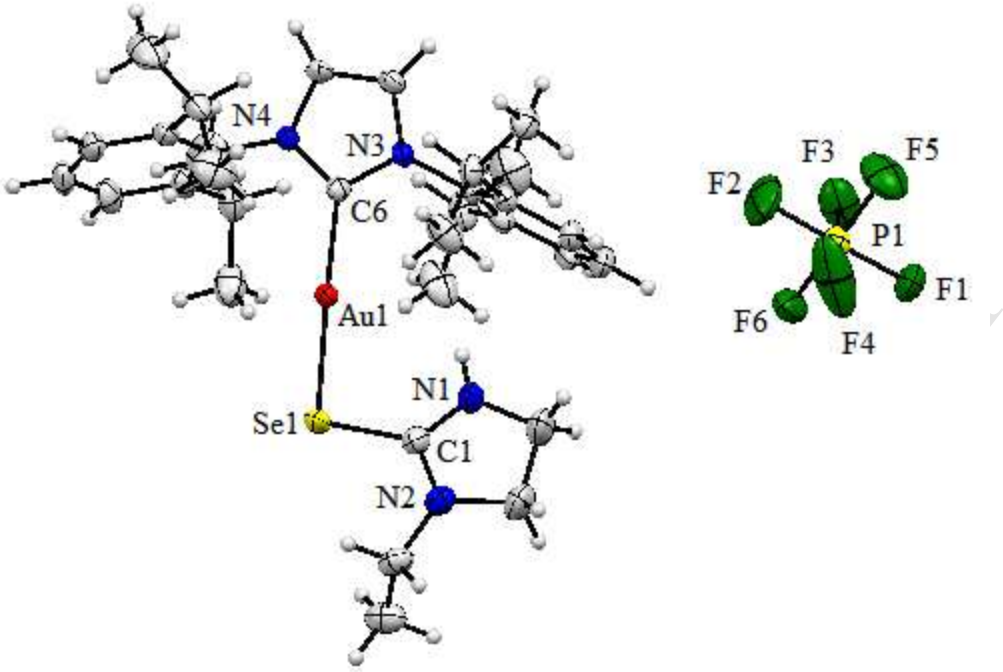

Figure 1 Molecular structure of complex [Au(IPr)(EtImSe]PF_6 (**2**) with partial labeling of atoms and 50% probability ellipsoids.

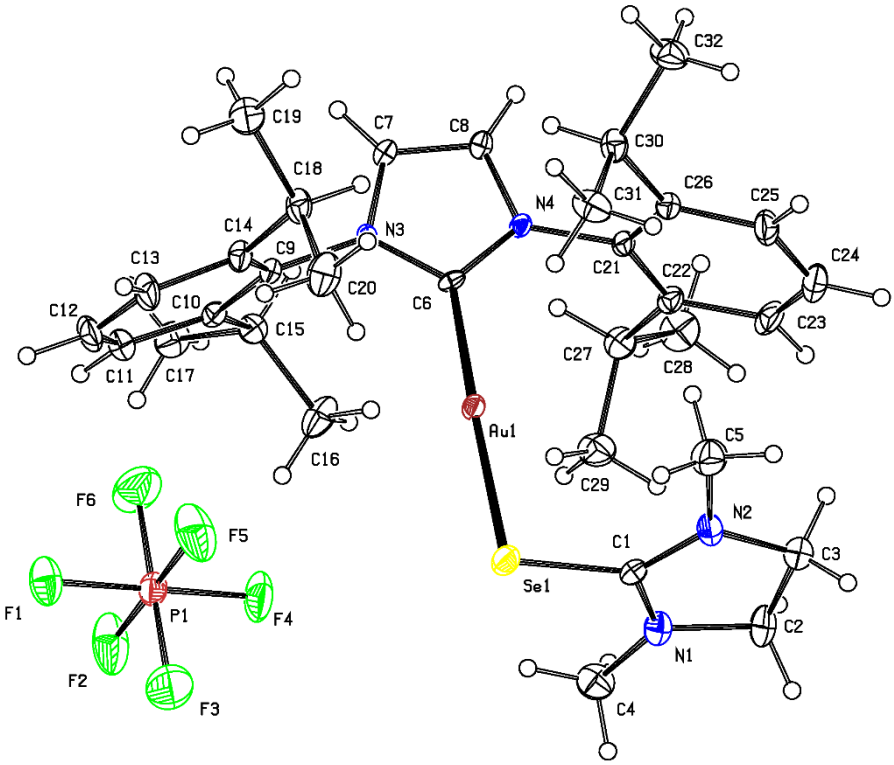

Figure 2 Molecular structure of complex [Au(IPr)(Me$_2$ImSe]PF_6 (**4**), with partial labeling of atoms and 50% probability ellipsoids.

269 Table 1 Selected bond distances (Å) and bond angles (˚) for compounds **2** and **4**

Bond Distance		Bond angles	
Compound **2**			
Au1—C6	2.009(2)	C6—Au1—Se1	176.82(6)
Au1—Se1	2.4030(3)	Au1—Se1—C1	98.61(8)
Se1—C1	1.868(3)	Au1—C6—N3	129.94(16)
N1—Cl	1.328(3)	N3—C6—N4	105.46(19)
N1—C2	1.456(4)	N1—C1— N2	110.9(2)
N3—C6	1.339(3)	N1—C1— Se1	126.4(2)
N3—C7	1.389(3)	N2—C1— Se1	122.68(19)
N3—C9	1.455(3)	C1—N1—C2	112.1(3)
		C6—N3—C7	110.89(19)
Compound **4**			
Au1—C6	2.015(6)	C6—Au1—Se1	176.76(17)
Au1—Se1	2.4068(8)	Au1—Se1—C1	95.2(2)
Se1—C1	1.899(7)	Au1—C6—N3	129.3(5)
N1—Cl	1.327(10)	N3—C6—N4	105.2(5)
N1—C2	1.469(10)	N1—C1— N2	111.9(7)
N3—C6	1.355(8)	N1—C1— Se1	124.0(6)
N3—C7	1.386(8)	N2—C1— Se1	124.0(6)
N3—C9	1.465(8)	C1—N1—C2	110.4(7)
		C6—N3—C7	110.5(5)

3.3. *In vitro* cytotoxic activities of gold(I) complexes (0-5)

Gold(I) complexes **(0-5)** were tested for *in vitro* cytotoxicity against A549 (human lung carcinoma), MCF7 (human breast adenocarcinoma) and HCT15 (human colon cancer) cell lines using MTT assay. Their activity was compared with the standard anticancer drug, cisplatin. The dose-dependent inhibition of cell proliferation was obtained by a specific increase in concentration of cisplatin and complexes **(0-5)** against a fixed number of three human cancer cell lines as shown in Figure 3. The IC_{50} values (μM) of cisplatin and complexes **(0-5)** against HCT15, A549 and MCF7 cancer cell lines are shown in Table 7. The data shows that the complex **1** is the most effective in inhibiting the growth of cancer cells. Its antiproliferative activity against HCT15 cells (IC_{50} 33 ± 1 μM) is almost equal to that of cisplatin (IC_{50} 32 ± 2 μM). All other studied gold complexes exhibit higher IC_{50} values and are therefore, less effective than cisplatin in inhibiting the growth of cancer cells. The poor activity of the complexes may be related to the strong binding of IPr and selenone ligands and their steric bulk.

Table 7 IC_{50} values (μM) of gold(I) complexes (**0-5**) against HCT15, A549 and MCF7 cancer cell lines.

Complex	HCT15	A549	MCF7
Cisplatin	32 ± 2	42 ± 2	23 ± 4
0	122 ± 1	180 ± 2	110 ± 2
1	33 ± 1	47 ± 1	43 ± 2
2	45 ± 1	56 ± 1	42 ± 1
3	62 ± 1	75 ± 1	53 ± 1
4	42 ± 1	58 ± 1	51 ± 1
5	51 ± 2	71 ± 1	51 ± 1

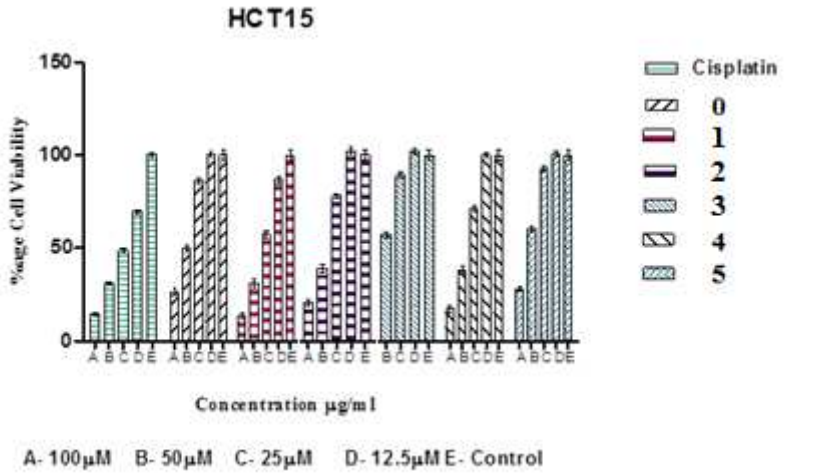

289
290

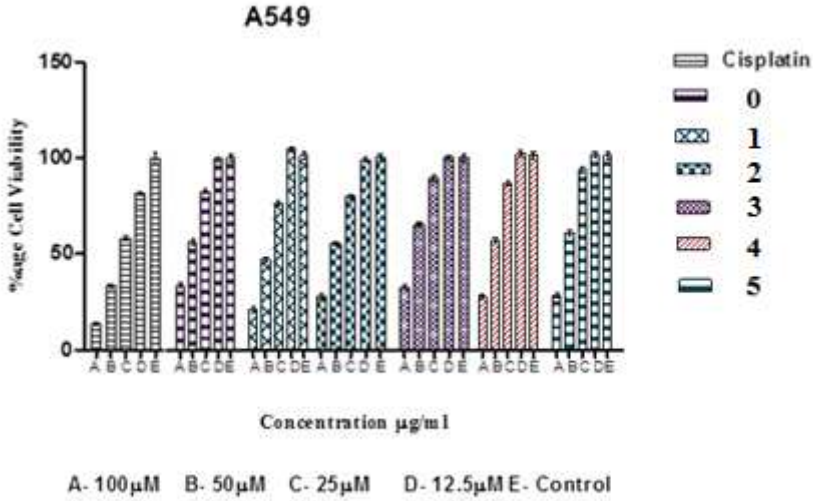

291
292

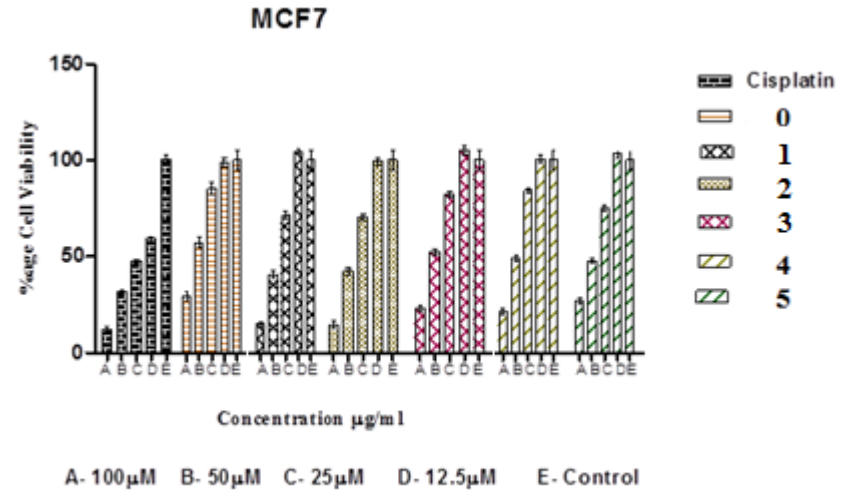

293

294 **Figure 3** Effect of concentration of complexes (cisplatin and **0-5**) on cell-viability of
295 different cell lines.

3.4. The Docking Studies of the Gold complexes with Thioredoxin Reductase

The docking studies of the synthesized gold(I) complexes were performed with the selenium-containing target protein, thioredoxin reductase (PDB ID: 3EAN) [60]. The protein was validated using the Ramachandran plot with the Moleman 2 [61] to check for the percentage outlier. For a valid protein, the percentage outlier should be between the range of 0 to 5 % [61]. The target protein proved to be valid by having a percentage outlier of 2.7 %.

Table 8 The docking results of gold(I) complexes (**1-5**) with human thioredoxin reductase-thioredoxin.

Compound	Molecular mass	HBD	HBA	cLogP	Rotatable bonds	Ro5 violation	Docking Score	Distance between Au and Sec 498(Å)
1	735.6	2	4	7.05	8	2	-25.75	6.638
2	763.7	1	4	6.87	9	2	-30.20	6.514
3	777.7	1	4	8.41	10	2	-33.87	6.413
4	763.7	1	4	7.67	8	2	-34.45	2.135
5	791.7	1	4	8.84	10	2	316	7.675

The CLC drug discovery workbench [62, 63] program was used to dock the gold complexes to the TrxR (PDB ID: 3EAN). However, the initial ligands were extracted from the target protein before being docked with the gold complexes. The active site in TrxR has been known to include Sec 498 (selenocysteine), which would lead to the formation of the gold-selenolate species [64-66]. The selenocyteine is known to undergo ligand exchange reaction upon interaction with gold(I) compounds [67].

The complexes were all minimized using Spartan 16 program [68] before being docked in the binding site. The Discovery studio program [69] was used to observe the binding mode and interactions present in the binding pocket of the docked results. Except for Sec 498, all other amino acid interactions present in the binding mode were discarded. The bond distance (Figures S1-S4) between the gold atom present in each complex and the selenium atom in the selenocysteine amino acid (Sec 498) was observed using the Gauss view program [70]. Complex **4** had the shortest distance of 2.13 Å (Fig. 4) between the gold

and selenium, which implied that it had the best potential to form the gold-selenolate species. This bond distance is in fact shorter than what was observed between Auranofin and selenocysteine [71] which is 5.897Å. All the complex showed negative docking scores except complex **5**, which implied that there was no binding affinity between the complex and the target protein (TrxR) since the more negative a docking score, the stronger the binding affinity. Moreover, the docking scores correlated with the bond distances between the gold and selenium atoms such that complex **4**, which possessed the shortest bond distance also had the highest docking score and same applied to complex **5** (Table 8). All the complexes violated the Lipinski's rule of five, by having a molecular mass and calculated logP (clogP) greater than 500 and 5 respectively. However, this does not deter them from being used as potential anticancer therapeutics since they can all be optimized into lead compounds [72, 73].

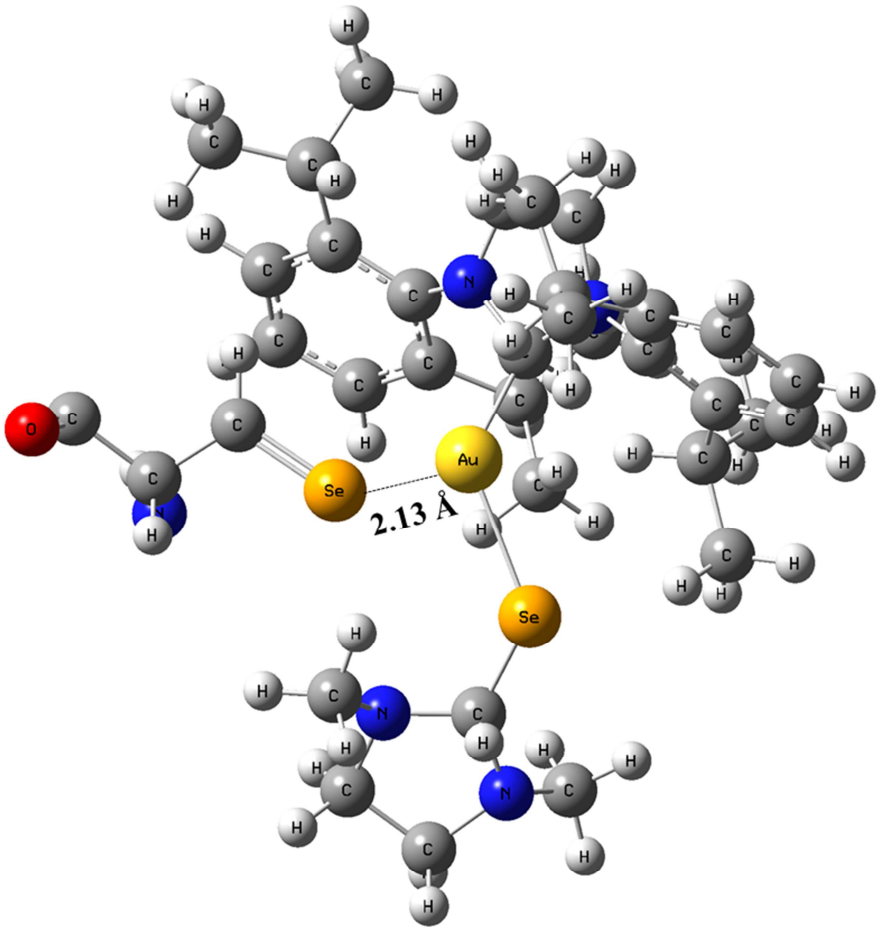

Figure 4. The interaction of complex **4** with Sec 498 in the binding site of TrxR (PDB ID: 3EAN).

3.5 Interaction of the Gold complexes with amino acids and protein

The interaction of the gold complexes was investigated with an amino acid and a protein. Different concentrations of the gold complexes were spiked into 0.5 mM tryptophan in 0.1 M PB to observe the interaction. All these complexes demonstrated a strong interaction with the tryptophan (Figs 5 and 5S). For instance, in the interaction of the complex **3** displayed in Figure 5 A, the tryptophan peak in absence of complex appeared at +0.708 V. Successive additions of complex **3** into the 0.5 mM tryptophan solution decreased the tryptophan oxidation peak current and shifted the peak potential towards more positive value. The peak potential of the tryptophan was shifted from +0.708 to +0.788 V by spiking 60 µM of complex **3**. Control experiments were also performed by spiking the same volume of solvent equivalent to the added volume of the complex into 0.5 mM tryptophan. In these control experiments, no peak shift was observed by spiking solvent blank, and only a small variation in current was observed (Fig. 5 A′), that has further validated the interaction of the complex **3** with tryptophan.

Interaction of the anticancer drugs was also investigated with the lysozyme protein. The electrochemical behavior of the lysozyme was also poor. However, a small peak of 0.2 mM lysozyme in 0.1 M acetate buffer appeared at +0.791 V. Interaction of the lysozyme was investigated with complex **3**. The change in peak current and the peak shift was observed by spiking various concentrations of the complex. However, the decrease in peak current and peak potential shift was not as prominent as observed with tryptophan. The lysozyme peak potential shifted from +0.791 to +0.816 V by spiking 60 µM complex **3** (Fig. 5 B). Similarly, a controlled experiment was run by spiking the same volume of the blank into lysozyme solution and no change in peak potential was observed. From this electrochemical study, it could be concluded that synthesized complexes were exhibiting the capability to interact with tryptophan and lysozyme.

The interaction of the other Gold complexes; **0**, **1**, **2**, **4** and **5** with tryptophan was also studied and results are shown in Fig. 5S. The spiking of any of all these drugs into 0.5 mM tryptophan solution caused a peak shift and a significant decrease in peak current (Fig. 5S).

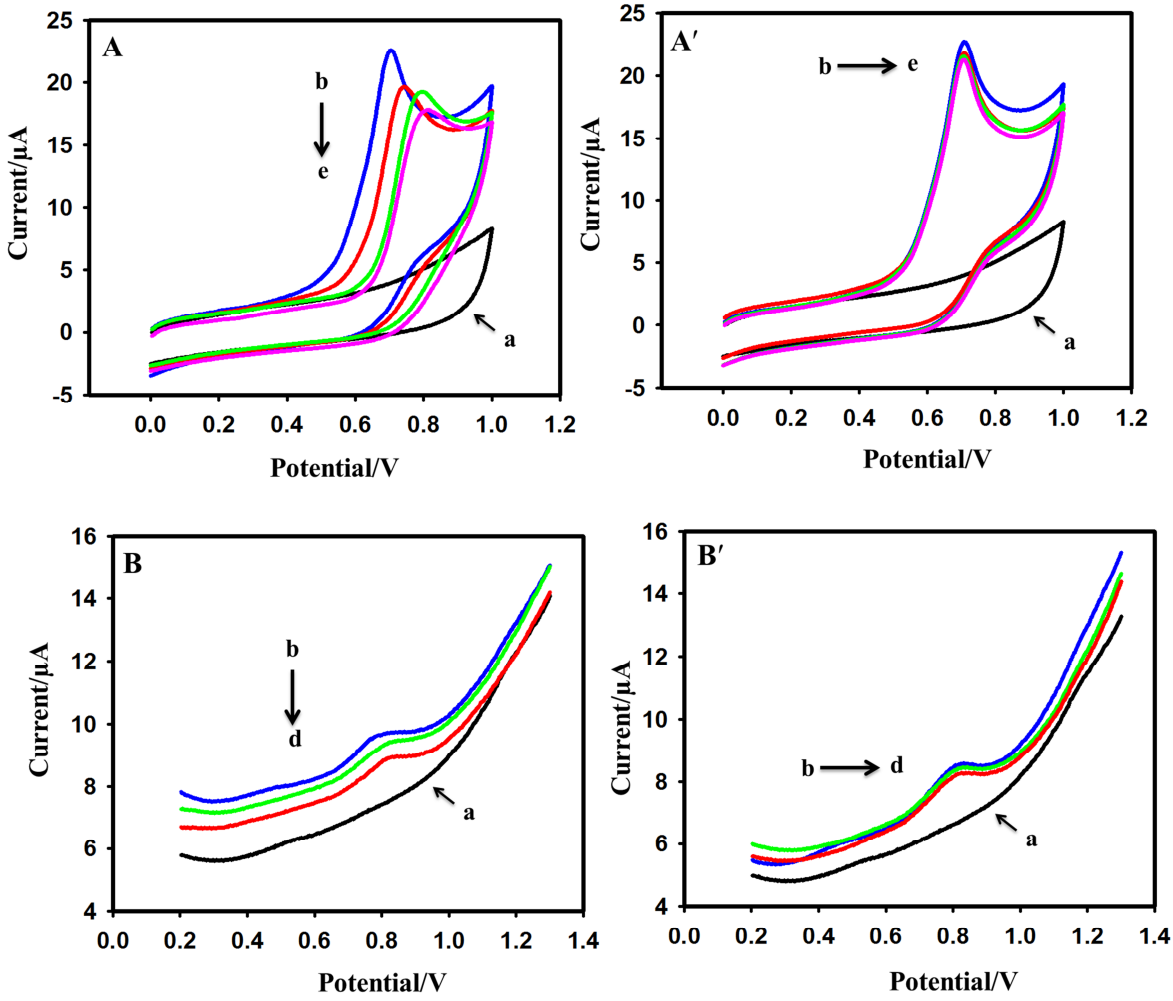

Figure 5. Cyclic voltammograms of the interaction of the complex **3** with 0.5 mM tryptophan (A) in 0.1 M PB (pH 6.8) at various concentrations of complex **3** (a) blank, absence of complex and tryptophan, (b) 0 µM (c) 20 µM, (d) 40 µM, (e) 60 µM. The response of 0.5 mM tryptophan solution in controlled experiment (A′) by adding solvent blank (b) 0 µL, (c) 30 µL, (d) 60 µL, (e) 90 µL. Square wave voltammograms of the interactions of the complex **3** with 0.2 mM Lysozyme (B) in 0.1 M acetate buffer (pH 4.7) at various concentrations of complex **3** (a) blank, absence of complex and lysozyme, (b) 0 µM (c) 40 µM, (d) 60 µM. The response of 0.2 mM lysozyme solution in controlled experiment (B′) by adding solvent blank (b) 0 µL, (c) 60 µL, (d) 90 µL.

Conclusion

We have synthesized five stable gold(I) carbene complexes with 1,3-imidazolidine-2-selenone and its derivatives. The X-ray structure of two complexes (**2** and **4**) are presented, which reveal a linear geometry about the gold(I) atom. The cytotoxic activities of the complexes were tested in three human cancer cell lines and only complex **1** was found to have activity comparable to cisplatin. The ducking studies indicated that complex **4** had the highest binding affinity (-34.45) and showed the molecular interactions such as, van der Waals, pi-cation and alkyl with the amino present in the target protein. Complex **4** has shortest bond distance between gold center atom and Sec 498 of TrxR (2.13 Å), while complex **5** has the highest (7.68 Å). The molecular docking results of the complexes with human thioredoxin reductase enzyme would be helpful to explore their mechanism of action. In the electrochemical experiments, the complexes were found to interact with tryptophan and the lysozyme protein. The oxidation peak potential of the tryptophan in presence of 60 µM complex **3** was shifted from +0.708 to +0.788 V. A similar behavior was observed for the lysozyme peak potential, which was shifted from +0.791 to +0.816 V in the presence of 60 µM complex **3.**

Acknowledgement

The authors greatly appreciate and thank the financial support provided by King Fahd University of Petroleum and Minerals under the project No. **IN151022.**

Supplementary information

CCDC numbers 1531011and 1531012 for the complexes **2** and **4** contain the supplementary crystallographic data for this paper. These data can be obtained free of charge from The Cambridge Crystallographic Data Centre via www.ccdc.cam.ac.uk/data_request/cif

References

1. J. Forestier, J. Lab. Clin. Med. 20 (1935) 827-840.
2. S.P. Fricker, Gold bulletin. 29 (1996) 53-60.
3. C. F. Shaw III, *Chem. Rev*., 1999, **99**, 2589-600.
4. S. Ahmad, A.A. Isab, S. Ali, A. R. Al-Arfaj, Polyhedron 25 (2006) 1633-1645.
5. W. Fiskus, N. Saba, M. Shen, M. Ghias, J. Liu, S.D. Gupta, L. Chauhan, R. Rao, S. Gunewardena, K. Schorno, C.P. Austin, K. Maddocks, J. Byrd, A. Melnick, P. Huang, A. Wiestner, K.N. Bhalla, Cancer Res. 74 (2014) 2520–2532.
6. X. Chen, X. Shi, C. Zhao, X. Li, X. Lan, S. Liu, H. Huang, N. Liu, S. Liao, D. Zang, W. Song, Q. Liu, B.Z. Carter, Q. P. Dou and X. Wang, J. Liu, *Oncotarget*, 2014, **5**, 9118–9132.
7. M. Altaf, M. Monim-ul-Mehboob, M.Ogasawara , N. Casagrande, M. Celegato, C. Borghese, Z.H. Siddik, D. Aldinucci, A.A. Isab, Oncotarget. 8 (2017) 490-505.
8. S.-H. G. Park, J.H. Lee, J.S. Berek and M. C.-T. Hu, Int. J. Oncol. 45 (2014) 1691–1698.
9. K.K. Ooi, C.I. Yeo, K.P. Ang, A.M. Akim, Y.K. Cheah, S.N.A. Halim, H.L. Seng, E.R.T. Tiekink, J. Biol. Inorg. Chem. 20 (2015) 855–873.
10. E. García-Moreno, S. Gascón, E. Atrián-Blasco, M.J. Rodriguez-Yoldi, E. Cerrada, M. Laguna, Eur. J. Med. Chem. 79 (2014) 164–172.
11. M. Altaf, M. Monim-ul-Mehboob, A.A.A Seliman, M. Sohail, M.I.M. Wazeer, A.A. Isab, L. Li, V. Dhuna, G. Bhatia, K. Dhuna, Eur. J. Med. Chem. 95 (2015) 464–472.
12. A.A.A. Sulaiman, M. Altaf, A.A. Isab, A. Alawad, S. Altuwaijri, S. Ahmad, Z. Anorg. Allg. Chem. 642 (2016) 1454–1459.
13. B. Bertrand, A. Casini, Dalton Trans. 43 (2014) 4209–4219.
14. J. Weaver, S. Gaillard, C. Toye, S. Macpherson, S.P. Nolan and A. Riches, Chem. Eur. J. 17 (2011) 6620 – 6624.
15. Y. Li, G.-F. Liu, C.-P. Tan, L.-N. Ji, Z.-W. Mao, Metallomics 16 (2014) 1460-1468.

16. B. Bertrand, A. Citta, I.L. Franken, M. Picquet, A. Folda, V. Scalcon, M.P. Rigobello, P. Le Gendre, A. Casini, E. Bodio, J. Biol. Inorg. Chem. 20 (2015) 1005–1020.

17. A. Pratesi, D. Cirri, M.D. Duovic, S. Pillozzi, G. Petroni, Z.D. Bugarcic, L. Messori, Biometals 29 (2016) 905-911.

18. P.J. Barnard, M.V. Baker, S.J. Berners-Price and A.D. Day, J. Inorg. Biochem. 98 (2004) 1642–1647.

19. R. Rubbiani, E. Schuh, A. Meyer, J. Lemke, J. Wimberg, N. Metzler-Nolte, F. Meyer, F. Mohr, I. Ott, Med. Chem. Commun. 4 (2013) 942-948.

20. E. Schuh, C. Pfluger, A. Citta, A. Folda, M.P. Rigobello, A. Bindoli, A. Casini, F. Mohr, J. Med. Chem. 55 (2012) 5518–5528.

21. L. Messori, L. Marchetti, L. Massai, F. Scaletti, A. Guerri, I. Landini, S. Nobili, G. Perrone, E. Mini, P. Leoni, M. Pasquali, C. Gabbiani, Inorg. Chem., 53 (2014) 2396–2403.

22. T.J. Siciliano, M.C. Deblock, K.M. Hindi, S. Durmus, M. J. Panzner, C. A. Tessier and W. J. Youngs, J. Organomet. Chem. 696 (2011) 1066–1071.

23. B. Bertrand, L. Stefan, M. Pirrotta, D. Monchaud, E. Bodio, P. Richard, P. Le Gendre, E. Warmerdam, M.H. de Jager, G.M.M. Groothuis, M. Picquet, A. Casini, Inorg. Chem. 53 (2014) 2296–2303.

24. H. Sivaram, J. Tan, H.V. Huynh, Organometallics 31 (2012) 5875-5883.

25. B.K. Rana, A. Nandy, V. Bertolasi, C.W. Bielawski, K.D. Saha, J. Dinda, Organometallics 33 (2014) 2544–2548.

26. M. Altaf, M. Monim-ul-Mehboob, A.A.A. Seliman, A.A. Isab, V. Dhuna, G. Bhatia, K. Dhuna, J. Organomet. Chem. 765 (2014) 68-79.

27. B. Bertrand, E. Bodio, P. Richard, M. Picquet, P. Le Gendre and A. Casini, J. Organomet. Chem. 775 (2015) 124-129.

28. M.V. Baker, P. J. Barnard, S.J. Berners-Price, S.K. Brayshaw, J.L. Hickley, B.W. Skelton, A.H. White, Dalton Trans. (2006) 3708–3715.

29. J. L. Hickey, R. A. Ruhayel, P. J. Barnard, M. V. Baker, S. J. Berners-Price and A. Filipovska, J. Am. Chem. Soc. 130 (2008) 12570-12571.

30. X. Cheng, P. Holenya, S. Can, H. Alborzinia, R. Rubbiani, I. Ott, S. Wolfl, Mol. Cancer 13 (2014) 221.

31. S.B. Aher, P.N. Muskawar, K. Thenmozhi, P.R. Bhagat, Eur. J. Med. Chem. 81 (2014) 408–419.

32. F. Hackenberg, H. Muller-Bunz, R. Smith, W. Streciwilk, X. Zhu, M. Tacke, Organometallics. 32 (2013) 5551-55560.

33. W. Walther, O. Dada, C. O'Beirne, I. Ott, G. Sánchez-Sanz, C. Schmidt, C. Werner, X. Zhu, M. Tacke, Lett. Drug Design & Discov. 14 (2017) 125-134.

34. M.V. Baker, P.J. Barnard, S.J. Berners-Price, S.K. Brayshaw, J.L. Hickey, B.W. Skelton, A.H. White, J. Organomet. Chem. 690 (2005) 5625–5635.

35. R. Rubbiani, S. Can, I. Kitanovic, H. Alborzinia, M. Stefanopoulou, M. Kokoschka, S. Mönchgesang, W.S. Sheldrick, S. Wölfl, I. Ott, J. Med. Chem. 54 (2011) 8646–8657.

36. M.Z. Ghdhayeb, R.A. Haque, S. Budagumpi, J. Organomet. Chem., 757 (2014) 42-50.

37. E. Deck, K. Reiter, W. Klopper, F. Breher, Z. Anorg. Allg. Chem. 642 (2016) 1320–1328.

38. M.R. Fructos, T.R. Belderrain, P. de Fremont, N.M. Scott, S.P. Nolan, M.M. Diaz-Requejo, P.J. Perez, Angew. Chem. Int. Ed. 44 (2005) 5284 –5288.

39. S. Gaillard, A.M.Z. Slawin, S.P. Nolan, Chem. Commun. 46 (2010) 2742–2744.

40. O. Schuster, L. Yang, H.G. Raubenheimer, M. Albrecht, Chem. Rev. 109 (2009) 3445-3478.

41. X. Xu, S.H. Kim, X. Zhang, A.K. Das, H. Hirao, S.H. Hong, Organometallics 32 (2013) 164–171.

42. D. Marchione, L. Belpassi, G. Bistoni, A. Macchioni, F. Tarantelli, D. Zuccaccia, Organometallics 33 (2014) 4200-4208.

43. D. Benitez, N.D. Shapiro, E. Tkatchouk, Y. Wang, W.A. Goddard, F.D. Toste, Nature Chem. 1 (2009) 482–486.

44. L.N.D.S. Comprido, J.E.M.N. Klein, G. Knizia, J. Kastner, A.S.K. Hashmi, Angew. Chem. Int. Ed. 54 (2015) 10336 –10340.

45. S. Ahmad, M.N. Akhtar, A.A. Isab, A.R. Al-Arfaj, M.S. Hussain, J. Coord. Chem. 51 (2000) 225-234.

46. S. Ahmad, A.A. Isab, A.R. Al-Arfaj and A.P. Arnold, Polyhedron 21 (2002) 2099-2105.

47. A. Ahmad, A.A. Isab, Trans. Met. Chem. 28 (2003) 540–543.

48. A.A. Isab, S. Ahmad, A. P. Arnold, Trans. Met. Chem. 29 (2004) 870–873.

49. M. Fettouhi, M.I.M. Wazeer, S. Ahmad, A.A. Isab, Polyhedron 23 (2004) 1–4.

50. M.I.M. Wazeer, A.A. Isab, S. Ahmad, J. Coord. Chem. 58 (2005) 391–398.

51. M.I.M. Wazeer, A.A. Isab, H.P. Perzanowski, Magn. Reson. Chem. 41 (2003) 1026–1029.

52. F.A. Devillanova, G. Verani, *Spectrochim.* Acta Part A Mol. Spectrosc. 36 (1980) 371–373.

53. G.M. Sheldrick, A short of SHELX, Acta Cryst. A64 (2008) 112-122.

54. G. M. Sheldrick, Crystal Refinement with SHELXL, Acta Cryst. C71 (2015) 3–8.

55. A.L. Spek, Acta Cryst. D65 (2009) 148-155.

56. A. A. Isab, M.I.M. Wazeer, M. Fettouhi, S. Ahmad, W. Ashraf, Polyhedron 25 (2006) 2629-2636.

57. A.O.S. Altoum, A. Alhoshani, K. Alhosaini, M. Altaf, S. Ahmad, S.A. Popoola, A.A. Al-Saadi, A.A. Sulaiman, A.A. Isab, J. Coord. Chem. 70 (2017) 1020-1031.

58. D.J. Nelson, F. Nahra, S.R. Patrick, D.B. Cordes, A.M.Z. Slawin, S.P. Nolan, Organometallics 33 (2014) 3640-3645.

59. M. T. Aroz, M. C. Gimeno, M. Kulcsar, A. Laguna and V. Lippolis, *Eur. J. Inorg. Chem.*, 2011, 2884–2894.

60. K. Fritz-Wolf, S. Kehr, M. Stumpf, S. Rahlfs, K. Becker, Nat. Commun., 2 (2011) 383–383.

61. G.J. Kleywegt, T.A. Jones, Structure 4 (1996) 1395–1400.

62. B. Li, S. Turuvekere, M. Agrawal, D. La, K. Ramani, D. Kihara, Proteins 71 (2008) 670-683.

63. B. Knudsen, K. Thomas, CLC Drug Discovery Workbench User Manual (2016) 1–367.

64. A. J. Freemerman, A. Gallegos, G. Powis, Cancer Res. 59 (1999) 4090–4094.

65. J.E. Oblong, M. Berggren, P.Y. Gasdaska, G. Powis, J. Biol. Chem. 269 (1994) 11714–11720.

66. P. K. Bhabak, J. B. Bhuyan, G. Mugesh, Dalton Trans. 40 (2011) 2099–2111.

67. S. Ahmad, A. A. Isab, M. I. M. Wazeer, Inorg. Reaction Mech., 4 (2002) 95-102.

68. Spartan 16. (n.d.) Irvine CA: Wavefunction Inc.

69. D. S. Biovia, Discovery Studio Modeling Environment. San Diego: Dassault Systèmes (2015).

70. J. Dennington, T. K. Millam, R. Dennington, T. Keith, J. Millam, GaussView. Shawnee Mission KS: Semichem Inc. (2009). (http://doi.org/10.1021/ja906885v).

71. T. Shoeib, D.W. Atkinson, B.L. Sharp, Inorg. Chim. Acta 363 (2010) 184–192.

72. C.A. Lipinski, F. Lombardo, B.W. Dominy, P. J. Feeney, Adv. Drug Deliv. Rev. 46 (2001) 3–26.

73. C.A. Lipinski, Adv. Drug. Deliv. Rev. 101 (2016) 34─41.

- Gold(I) complexes of the type C-Au(I)-Se were synthesized.
- Cytotoxicity of complexes measured against HCT15, A549 and MCF7 cell lines.
- X-ray data shows the gold coordination sphere adopts a linear geometry